OCEANS AND ATMOSPHERE
www.csiro.au

Sea-Level Rise and Allowances for Tasmania based on the IPCC AR5

Kathleen L. McInnes, Didier Monselesan, Julian O Grady, John Church and Xuebin Zhang

15 May 2016

Report for Tasmanian Department of Premier and Cabinet

Oceans and Atmosphere

Citation

McInnes KL, Monselesan D, O'Grady JG, Church JA and Xhang, X, 2016: Sea-Level Rise and Allowances for Tasmania based on the IPCC AR5, CSIRO Report 33 pp.

Copyright

© Commonwealth Scientific and Industrial Research Organisation 2015. To the extent permitted by law, all rights are reserved and no part of this publication covered by copyright may be reproduced or copied in any form or by any means except with the written permission of CSIRO.

Important disclaimer

CSIRO advises that the information contained in this publication comprises general statements based on scientific research. The reader is advised and needs to be aware that such information may be incomplete or unable to be used in any specific situation. No reliance or actions must therefore be made on that information without seeking prior expert professional, scientific and technical advice. To the extent permitted by law, CSIRO (including its employees and consultants) excludes all liability to any person for any consequences, including but not limited to all losses, damages, costs, expenses and any other compensation, arising directly or indirectly from using this publication (in part or in whole) and any information or material contained in it.

CSIRO is committed to providing web accessible content wherever possible. If you are having difficulties with accessing this document please contact enquiries@csiro.au.

Photo credit

Ocean Beach near Grantville Harbour: Mark Hemer

Contents

Figures

Tables

1 Introduction

This report provides information on updated projections of sea-level rise and water level allowances that have been developed for the Tasmanian Department of Premier and Cabinet. The updated values are consistent with those developed for the National Resource Management Project, available at http://www.climatechangeinaustralia.gov.au/en/climate-projections/coastal-marine/marine-explorer/ (see also McInnes et al., 2015) and the IPCC (Church et al., 2013a, b) and the NCCARF CoastAdapt web portal. The information presented here has been adapted to the requirements of the Tasmanian Department of Premier and Cabinet by adjusting the values to a reference year of 2010 (as opposed to the 1986-2005 average used by the IPCC, NRM and McInnes et al, 2015). The results presented here update a previous assessment undertaken by the Tasmanian Climate Change Office (2012) to provide sea-level projections and water level allowances based on the IPCC Fourth Assessment report (AR4) (IPCC, 2007). The report also provides information to aid in the interpretation and use of the sea-level rise projections and allowances data sets.

Information on extreme sea-level likelihoods is necessary for the assessment of exposure and vulnerability from rising sea levels due to global warming. Assessments of exposure and vulnerability are commonly generated from flood mapping using hydrodynamic and/or wave models (Hoeke et al, 2015) or Geographic Information Systems (e.g. Department of Climate Change, 2009, Lacey et al, 2015) or a combination of both (McInnes et al, 2012a, 2013). The common practice is to investigate flooding from an extreme sea-level height associated with a particular annual exceedance probability AEP such as a 0.01AEP (e.g. a 1 - in - 100 year sea level) combined with sea-level rise (SLR) projected for selected future times.

This report provides information on the derivation of updated sea-level rise projections and allowances for the Tasmanian Department of Premier and Cabinet. The report also discusses the historical context for sea-level rise in Australia, the projections, sea-level allowances and how to use them. Sea-level rise projections and allowances are provided as coastal council-averaged and state-averaged values in this report as well as continuous coastal data in accompanying datasets.

2 Understanding Sea-level Rise and Variability

Sea levels change on a broad range of time and space scales. These time-scales range from seconds for surface waves, to hours/days for tides and storm surges, days/months/years/decades and longer for regional variability, seasonal variations, natural climate variability and the response to anthropogenic climate change. On a global scale, anthropogenic climate change is causing an increase in the volume of the ocean (and a rise in global mean sea level; Figure 1) through the expansion of ocean waters as they warm and an increase in mass of the ocean as glaciers and ice sheets lose mass (Church et al., 2013a). The mass of the ocean also changes as water is exchanged with terrestrial environment from the impacts of climate variability and change and through anthropogenic activities such as the storage of water in reservoirs and the depletion of groundwater (which subsequently makes its way to the ocean).

Locally, sea-level changes not only because of the global change in volume of the ocean but also from a series of regional factors. Changes in regional sea level are dynamically linked to local and regional changes in the density of the ocean (which is dependent on temperature and salinity) and changes in ocean currents and as a result of air-sea interactions (winds and fluxes of heat and freshwater between the oceans and the atmosphere). Because of the dynamical coupling, changes in sea level at one location are linked to changes elsewhere in the ocean. For example, during El Niño events that bring drought to Australia, sea level is high in the eastern equatorial Pacific and low in the western equatorial Pacific, with the opposite occurring during La Niña events. The Interdecadal Pacific Oscillation and other climatic modes of variability affect regional sea level at higher latitudes and generally on longer decadal time scales. As water is added to the ocean, the sea-level signal propagates rapidly (within days) around the globe such that sea level also rises at locations distant from the initial mass addition (Lorbacher et al. 2012).

Sea level relative to the land (relative sea level, as measured by a coastal tide gauge) also changes if the land is moving. This land motion can occur because of ongoing global scale movements of the land in response to changes in the distribution of ice on the Earth since the last ice age (the last glacial maximum occurred about 20 thousand years ago), or local land motion associated with earthquakes or other tectonic effects such as sediment compaction (particularly in deltaic regions and where ground water or petroleum is withdrawn from the sediments). Contemporary changes in the mass of glaciers, ice sheets and the terrestrial storage of water also change the gravitational field and rotation of the Earth resulting in a global redistribution of sea level (a greater than average relative rise far from the region of loss of mass and a reduced rise and even a fall in relative sea level close to the region of loss of mass). In contrast to tide gauges, satellite measure sea level relative to the centre of mass of the Earth/ocean/ice system (geocentric sea level).

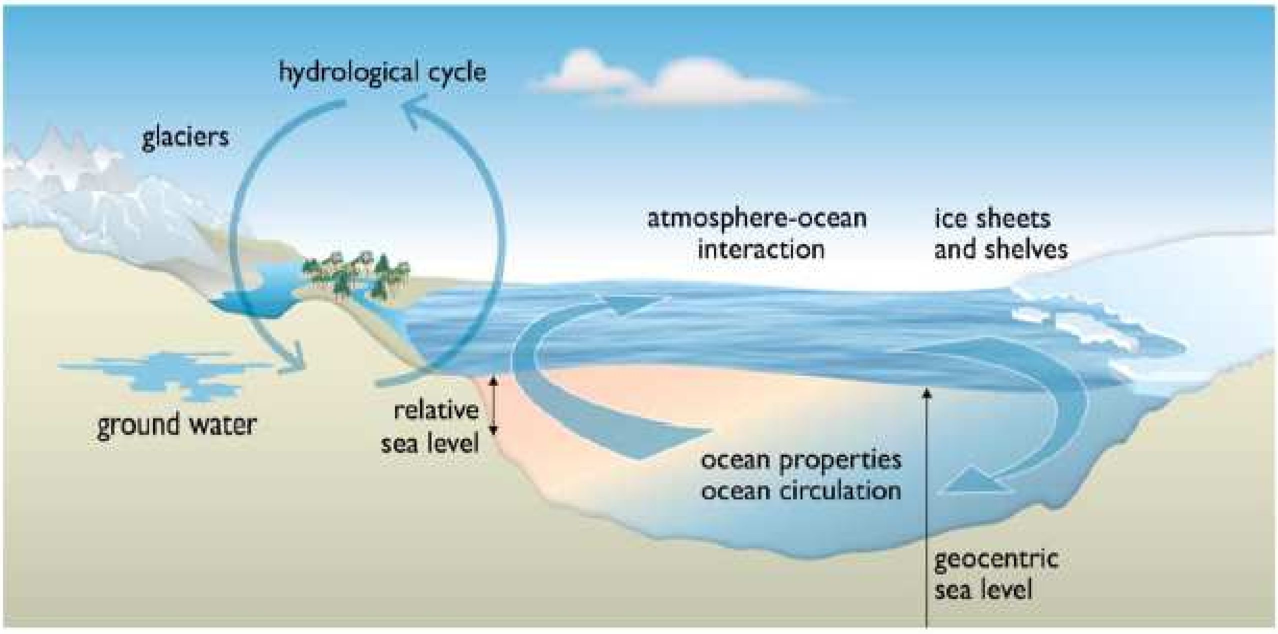

Figure 1. Climate-sensitive processes and components that can influence global and regional sea level. The term 'ocean properties' refers to ocean temperature, salinity and density, which influence and are dependent on ocean circulation (source: Church et al., 2013a).

Sea levels along most sections of the Australian coastline have been observed since 1966. There is significant interannual variability, much of which is related to the Southern Oscillation Index (SOI; White et al. 2014) and the Interdecadal Pacific Oscillation (Zhang and Church 2012). White et al. (2014) removed the variability directly related to the SOI and for the periods 1966 to 2009 and 1993 to 2009 estimated the average trends of relative sea level around the coastline of 1.4 ± 0.3 mm yr^{-1} and 4.5 ± 1.3 mm yr^{-1} (with the largest rates in this latter period on the north and west coasts of Australia). These rates became 1.6 ± 0.2 mm yr^{-1} and 2.7 ± 0.6 mm yr^{-1} after the signal directly correlated with ENSO was removed. After further correcting for GIA and changes in atmospheric pressure (Figure 2), they found the corresponding trends were 2.1 ± 0.2 mm yr^{-1} and 3.1 ± 0.6 mm yr^{-1}, with the average close to the global-mean trends, including the increased rate of rise since the early 1990s. For Australia's two longest records (Fremantle and Sydney), they found both records showing larger rates of rise between 1920 and 1950, relatively stable mean sea levels between 1960 and 1990 and an increased rate of rise from the early 1990s.

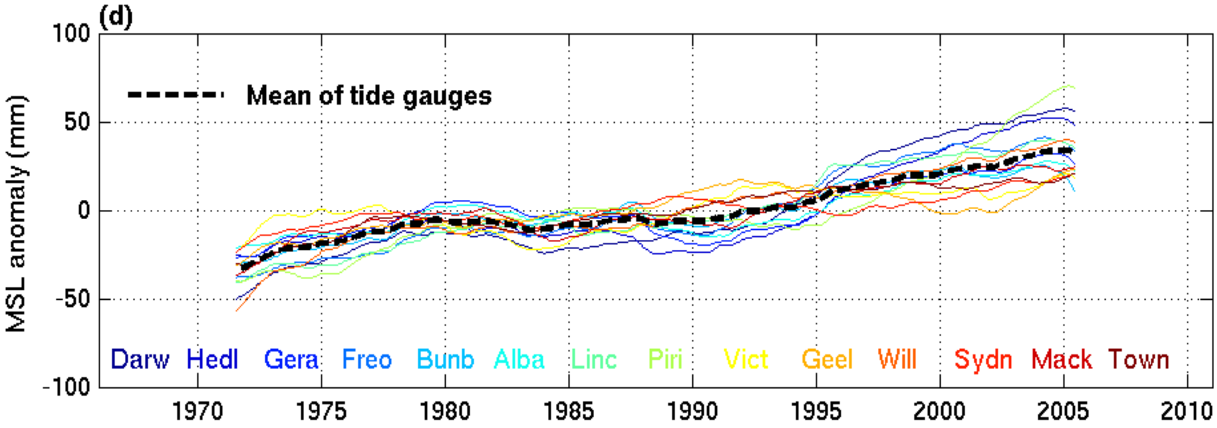

Figure 2. The tide gauge data (after the signal linearly correlated with the SOI has been removed and the results smoothed with a ten year running average) for the 14 tide-gauge records (different colours) and the average (black dashed; source: White et al., 2014).

Over the last five years there has been significant progress in providing a quantitative explanation for the observed sea-level rise from observations of the individual contributions, particularly since 1970 when more data are available (Church et al. 2011a; Moore et al. 2011), and also since 1900 using a combination of observations and models (Gregory et al. 2012; Church et al. 2013a,b). The two largest contributions come from ocean thermal expansion and the loss of mass from glaciers. The surface mass balance (SMB) of Greenland has been making an increasing contribution to sea-level rise since 1990. Part of this Greenland SMB contribution since 1990 appears to be related to anthropogenic climate change with part related to natural variability in the North Atlantic region (Church et al. 2013a).

The contributions from the ice sheets of Greenland and Antarctica related to rapid changes in discharge of ice into the oceans remains poorly determined, although it is thought that the 20th century contribution is small (Kjeldsen et al. 2015). There are now observations of the total mass balance changes of both ice sheets since the early 1990s using multiple techniques (Shepherd et al. 2012) and new models of the projected ice discharge for the 21st century for both the

Greenland (Nick et al. 2013) and Antarctic ice sheets (Levermann etal. 2014; Favier et al. 2013; Cornford et al., 2015; Ritz et al. 2015; De Conto and Pollard 2016).

There are also long term (and non-trivial) contributions from the depletion of ground water (Konikow 2011; Wada et al. 2012) and the storage of water in reservoirs (Chao et al. 2008; updated by Wada et al. 2012). The storage of water on land related to natural variability is thought to be small over multidecadal periods (Ngo-Duc et al. 2005) but it is becoming increasingly clear that it is important over multi year periods (Boening et al. 2012; Dieng et al. 2015; Reager et al. 2016).

When models of all of these contributions are combined there is now reasonably good agreement between the simulated and observed global mean sea level, especially since 1970 and 1993 when improved observations are available

Recent attribution studies have demonstrated that natural climate forcing or variability cannot explain the observed trend in ocean thermal expansion since 1970, although it is responsible for some of the decadal variability (Slangen et al. 2014). The modelled response from the combined climate forcing from greenhouse gases and aerosols is in reasonable agreement with the observed trend since 1970 (Marcos and Amores 2014; Slangen et al. 2014). For the glacier contribution, Marzeion et al. (2014) demonstrated that the response to past climate variations was an important contribution to the glacier contribution in the first half of the 20th century, but that anthropogenic forcing was responsible for the majority of the glacier contribution during the latter half of the 20th century.

Slangen et al. (2016) completed a comprehensive analysis of the causes of 20th century global mean sea-level (GMSL) rise. They found that the sum of all modelled contributions explains 74 ± 22% (± 2σ) of the observed GMSL change over 1900-2005. Natural radiative forcing makes little contribution over the 20th century but combined with the ongoing response to past climatic variations explains 67 ± 23% of the observed rise prior to 1950, but only 9 ± 18% after 1970. In contrast, the anthropogenic forcing (primarily a balance between a positive sea-level contribution from greenhouse gases (GHG) and a partially offsetting component from anthropogenic aerosols) explains only 15 ± 55% of the observations before 1950, but increases to become the dominant contribution to sea-level rise after 1970 (69 ± 31%).

While uncertainties remain, particularly for the first half of the 20th century, the ability to explain the observed GMSL changes and the reasons for these changes gives greater confidence in our understanding of sea-level change and our ability to project future change.

3 Projections of Global Mean and Regional Sea-level Rise

The improved understanding of 20th century sea-level rise and the factors leading to the regional differences in the rate of rise has led to the development of and improved confidence in techniques for projection of the global averaged and the regional distribution of sea-level rise for the 21st century (Slangen et al. 2012; Church et al. 2011b). As a result, the Intergovernmental Panel on Climate Change provided probabilistic regional projections of sea-level rise for the first time in the Fifth Assessment Report (AR5; Church et al. 2013a,b). The regional projections for Australia presented here are based on the AR5 projections and the regional application of these are reported in McInnes et al. (2015).

The AR5 projections use scenarios of atmospheric greenhouse gas concentrations (Representative Concentration Pathways, RCPs) that range from high concentrations representing continued growth of emissions in a business-as-usual fashion (RCP8.5), to lower concentrations representing very strong mitigation and removal of carbon dioxide from the atmosphere in the second half of the 20th century (RCP2.6) and two intermediate scenarios (RCP4.5 and RCP6.0; the number is the approximate radiative forcing in W m^{-2} from greenhouse gas increases by 2100). Note that of these four scenarios, only RCP2.6 is projected to result in a warming that is *likely* (66% probability) to be less than 2°C above preindustrial temperatures.

The RCP's used in the AR5 replaced the SRES emission scenarios (Nakicenovic et al, 2000) used in the AR4 (IPCC, 2007). The atmospheric greenhouse gas concentrations from three of the four RCP's considered here follow similar trajectories to certain SRES emission scenarios. In particular, RCP8.5 maps closely onto the SRES A1FI scenario. RCP6.0 is similar to A1B although concentrations rise more slowly and attain higher overall concentrations. In RCP4.5 atmospheric concentrations of greenhouse gases are projected to rise faster up to 2050 before plateauing to values at around 2100 that are similar in magnitude to the SRES B1 scenario. There is no counterpart for the strong mitigation scenario, RCP2.0 amongst the SRES scenarios.

3.1 Global Projections

To estimate future sea-level changes, projected contributions from changes in ocean density and circulation (available directly from available climate models) are combined with additional sea-level contributions from the loss of mass from glaciers, the surface mass balance of the Greenland ice sheet and the dynamic response of the Greenland and Antarctic ice sheets and changes in land water storage (Church et al., 2013a). How these contributions and associated uncertainties are combined to form global mean sea level can be found in the supplementary materials of chapter 13 of the IPCC Fifth Assessment Report (Church et al., 2013a).

The contributions to global mean sea-level change for the four greenhouse gas RCPs are given in Figure 3. Projected global mean SLR by 2100 relative to 1986–2005 varies from 28–61 cm for the RCP 2.6 (strong mitigation scenario) to 52–98 cm for the RCP 8.5 (high emissions scenario), where the range for each scenario was estimated to be *likely* (covering 66% of the probabilities). For RCP 8.5 and 6.0, the rate of GMSL rise increases throughout the 21st century, whereas for RCP 2.6 and 4.5, the rate of rise decreases after about 2030 and 2070, respectively. A larger global mean SLR could occur prior to 2100 as a result of the marine ice sheet instability of the West Antarctic Ice Sheet (Church et al., 2013a; Rignot et al., 2014), but there was insufficient scientific evidence at the time of the AR5 to assign a specific likelihood to values larger than the *likely* range defined above. Any additional contribution from the potential collapse of marine-based sectors of the Antarctic Ice Sheet, if initiated, was assessed to not exceed several tenths of a metre of SLR by 2100 (Church et al., 2013a). Recent observations (Rignot et al., 2014) indicate increased loss of ice from west Antarctica and recent modelling (e.g. Favier et al., 2014; Joughin et al., 2014; Levermann et al. 2014; Cornford et al. 2015; Ritz et al. 2015) simulates increased outflow from the Antarctic Ice Sheet. Projections of mass loss in these studies increases confidence in the *likely* Antarctic contribution used in the IPCC AR5 and reduces the probability of a rise above this range (Clark et al. 2015). Nevertheless, understanding of the relevant ocean-ice sheet processes (Alley and Joughin, 2012; Willis and Church, 2012) is still incomplete and a higher sea-level rise is possible. Indeed, recently De Conto and Pollard (2016) simulated the collapse of Antarctic ice shelves as the result of surface melting and hydrofracturing, resulting in a sea-level rise for climate projections from one model at the upper end and even beyond the several tenths of a metre in the IPCC Assessment.

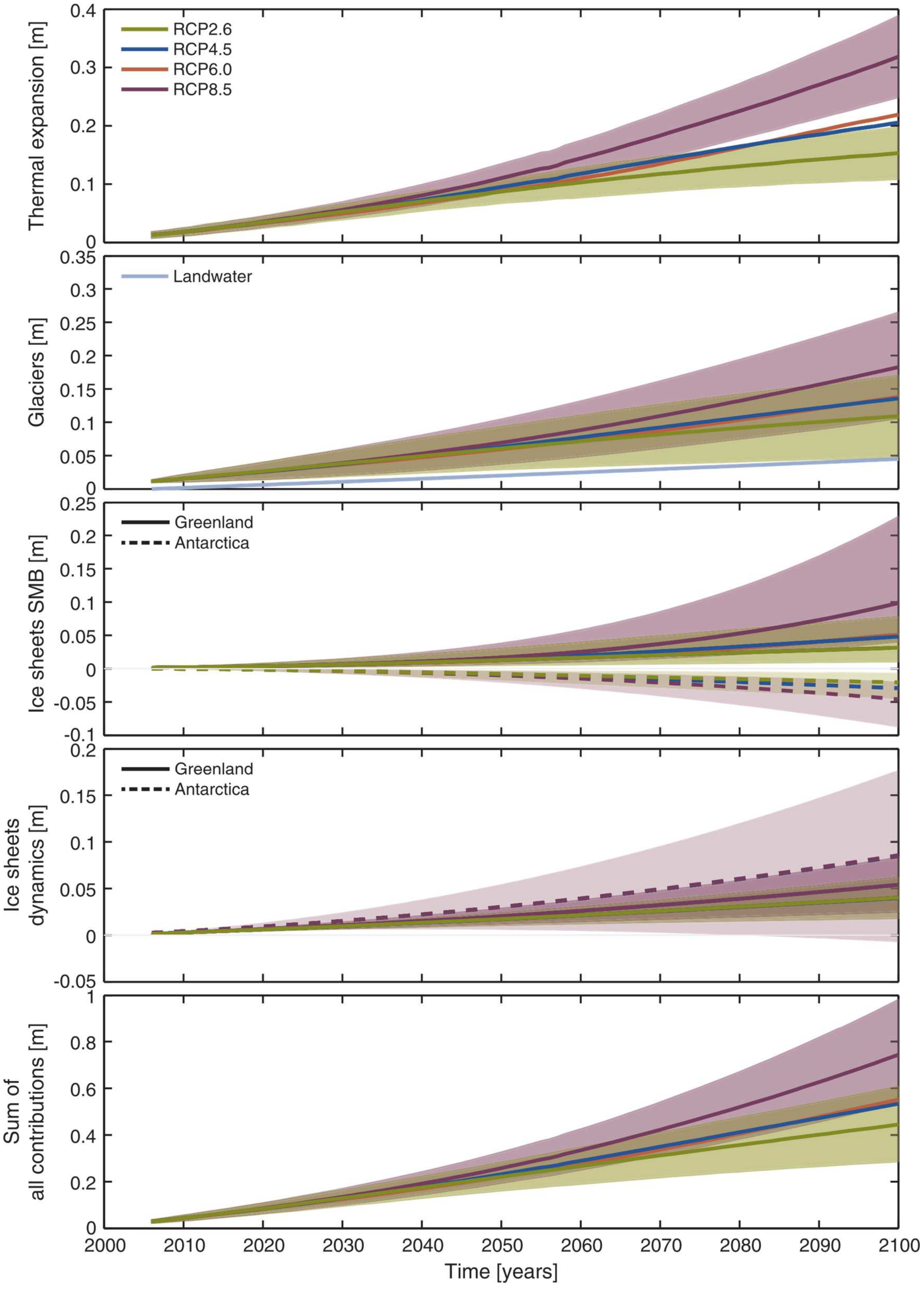

Figure 3. Contributions to 21st century sea-level rise (thick coloured lines) calculated using the results of individual climate models for all four RCPs. (a) Global-averaged ocean thermal expansion. (b) Glacier mass loss (c) Changes in the surface mass balance of the Greenland and Antarctic ice sheets, (d) Ice sheet dynamical contributions (e) the sum of all contributions. For the RCP 8.5 and RCP 2.6 scenarios the multi-model mean values with 5 to 95% model ranges (shaded areas) are shown but for RCP 6.0 and RCP 4.5 scenarios, only multi-model mean values are shown (source: McInnes et al., 2015).

3.2 Sea-level Projections for Australia

To determine the regional changes in sea level around the Australian coastline, McInnes et al. (2015) combined the global mean change with the dynamic ocean sea-level distribution (changes in sea level from ocean-circulation changes), regional changes associated with contemporary changes in mass of glaciers and ice sheets and the gravitational and rotational response in the ocean, and an ongoing GIA from the visco-elastic response of the Earth to the redistribution of ice-sheet mass since the last glacial maximum (Church et al., 2011b, 2013a; Slangen et al., 2012; 2014b).

Each of the components associated with a change in mass implies changes in the Earth's gravitational field and vertical movement of the crust (sea-level fingerprints). The resulting 'fingerprints' of sea-level change consist of a larger than global average rise far from the regions of mass loss and a sea-level fall in the immediate vicinity of the regions of mass loss. The Greenland fingerprint around the Australian coastline is insensitive to details of the exact location of mass loss from the Greenland Ice Sheet. For Antarctica, McInnes et al. assumed that the mass gain from increased accumulation of snow is uniformly distributed over the continent whereas the dynamic loss is expected to be from the West Antarctic Ice Sheet. The projected small changes in the mass of water stored on land in reservoirs and aquifers were assumed to result in a uniform change in sea level around the globe.

Note the regional projections of McInnes et al. are slightly different to those in Church et al. (2013b) in that they are low pass filtered (by averaging 21 years of results) to focus on the climate change signal, use a different model for estimating the GIA (from the pseudo-spectral algorithm of Kendall et al. (2005) which takes into account time-varying shorelines, changes in the geometry of grounded marine-based ice, and the feedback into sea level of Earth's rotation changes, and the ice-load history is from the ICE-5G model (Peltier, 2004)). McInnes et al. did not include the impact of projected changes in atmospheric pressure, likely to have an impact at about the 1-cm level over Australia. These and other minor differences in the way regional sea levels are computed are likely to result in only trivial differences between the projections of McInnes et al. (2015) and Church et al. (2013a,b).

3.1 Sea-level Projections for Tasmania

Sea-level projections are developed for the Tasmanian coastal councils (Figure 4). They differ from those presented in McInnes et al, (2015) with respect to the sea-level baseline. The projected sea-level rise in Church et al, (2013a) and McInnes et al, (2015) was relative to the average of the 1986 to 2005 period, i.e. approximately relative to 1995. In this study, the reference period is 2010. Sea-level projections and allowances centred on 2010 (i.e. A 21-year averaged over the period 2000-2020) are derived from the projections with respect to 1995 by zeroing the lower, median, upper percentiles time series in 2010 assuming that the adjustments (i.e. 2010 percentiles values measured with respect to the 1995 baseline) are time-independent. In other words the projection percentile rates are kept invariant with respect to the change of baseline. This an approximation: a proper change of baseline would require all components contributing to the total sea-level change and their associated uncertainties to be available so that they could be combined via a Monte-Carlo sampling approach as described in the IPCC AR5 Chapter 13 Supplementary material (AR5 13SM). However, we do not have access to the individual sea-level contributions and (non-linear) parametrisations as a function of baseline and therefore opted for the simple adjustment approach outlined here. We do not expect our approach will lead to significant differences particularly towards 2100.

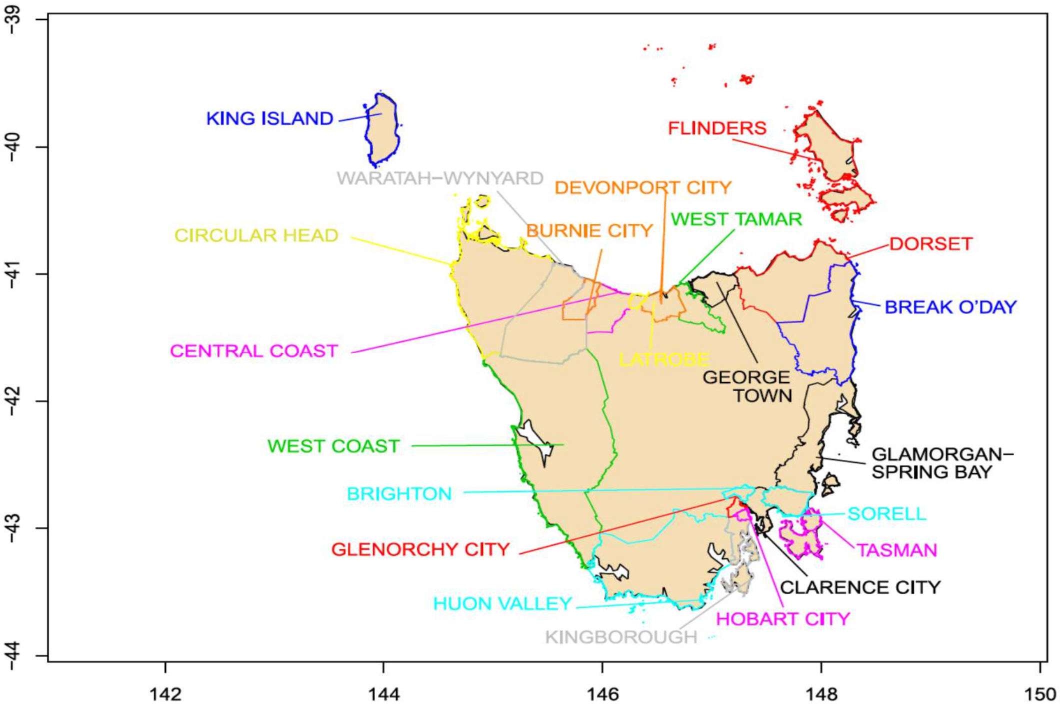

Figure 4. Coastal council boundaries in Tasmania.

The projected mid-range and 95th percentile sea-level rise for Tasmania is illustrated in Figure 5 for 2100 based on RCPs 4.5 and 8.5. Values vary around the coastline with the largest values occurring on the east coast. As shown in McInnes et al (2015) larger values occur off the east coast, which are related to the strengthening of the subtropical gyre circulation of the South Pacific Ocean (see also Zhang et al. 2014). This pattern intensifies with higher emissions. However the current low-resolution models may not adequately represent how these higher offshore sea levels are expressed at the coast. Present indications are that intensification of the East Australian Current (EAC) at least partially prevents these larger offshore anomalies from reaching the coast. The effect of GIA is to slightly lower relative rise along the Australian coastline compared to offshore.

Projected time series for the four RCPs are shown for selected coastal councils in Figure 6 and numerical values in Table 2. The global and regional projections are almost independent of the RCP chosen for the first decades of the 21st century, but they begin to differ significantly from about 2050. Significant interannual variability of monthly regional sea levels (as seen in the observations) has been effectively removed in forming the ensemble-average projections and the low-pass filtering. However, the interannual variability will likely continue through the 21st century and beyond. An indication of its magnitude is given by the dashed lines plotted above the top and below the bottom of the projections in Figure 7 indicating the 5 to 95 percent uncertainty range of the detrended historical records.

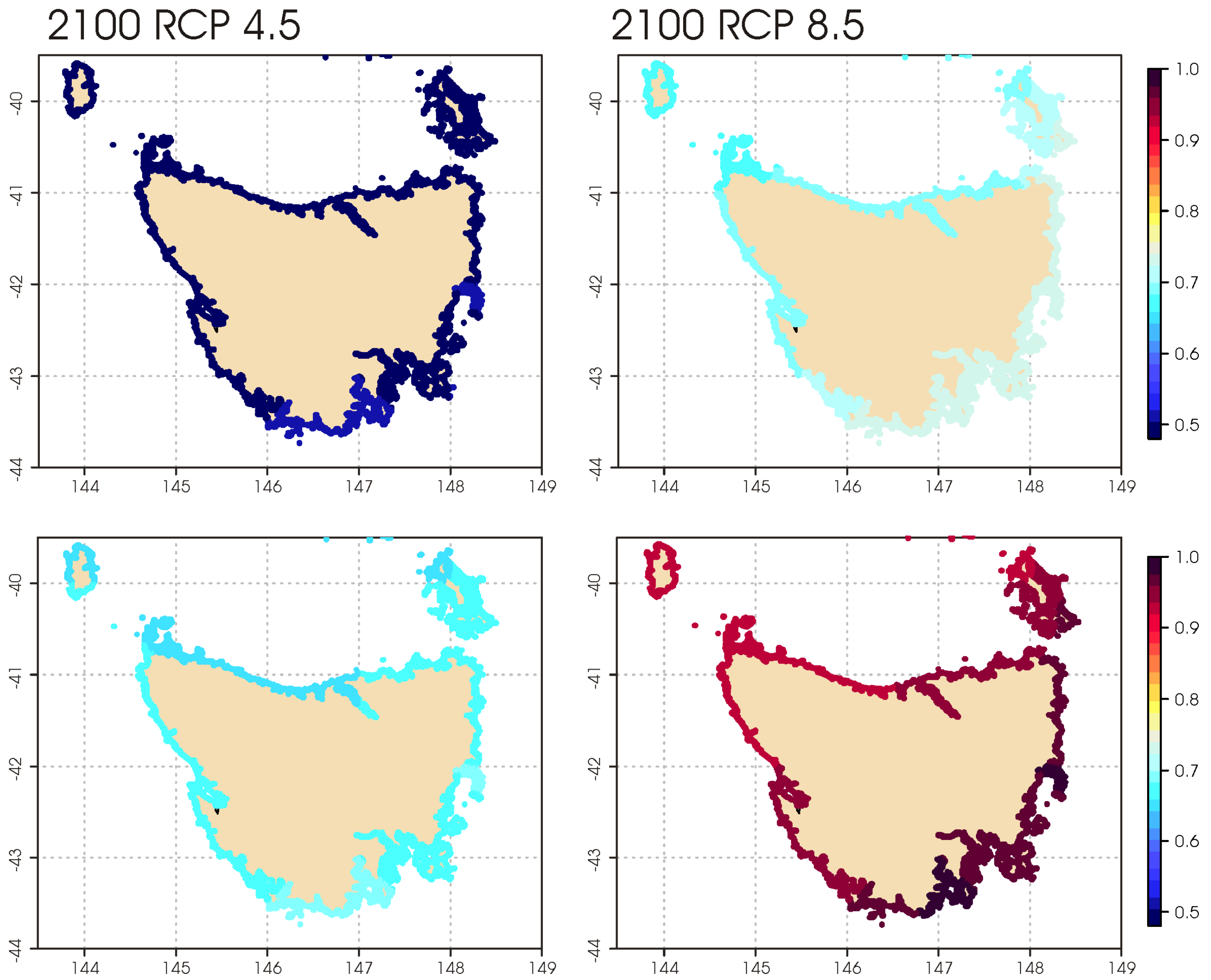

Figure 5. Projected median sea-level change (top) and 95th percentile of sea level change (bottom) in 2100 around the coastline of Tasmania for RCP 4.5 (left) and RCP 8.5 (right) relative to 2010. Units are m. The values include the thermal expansion component derived from CMIP5 AOGCMs, the contributions from the changes in terrestrial ice, the gravitational response of the ocean to these changes, and an ongoing GIA.

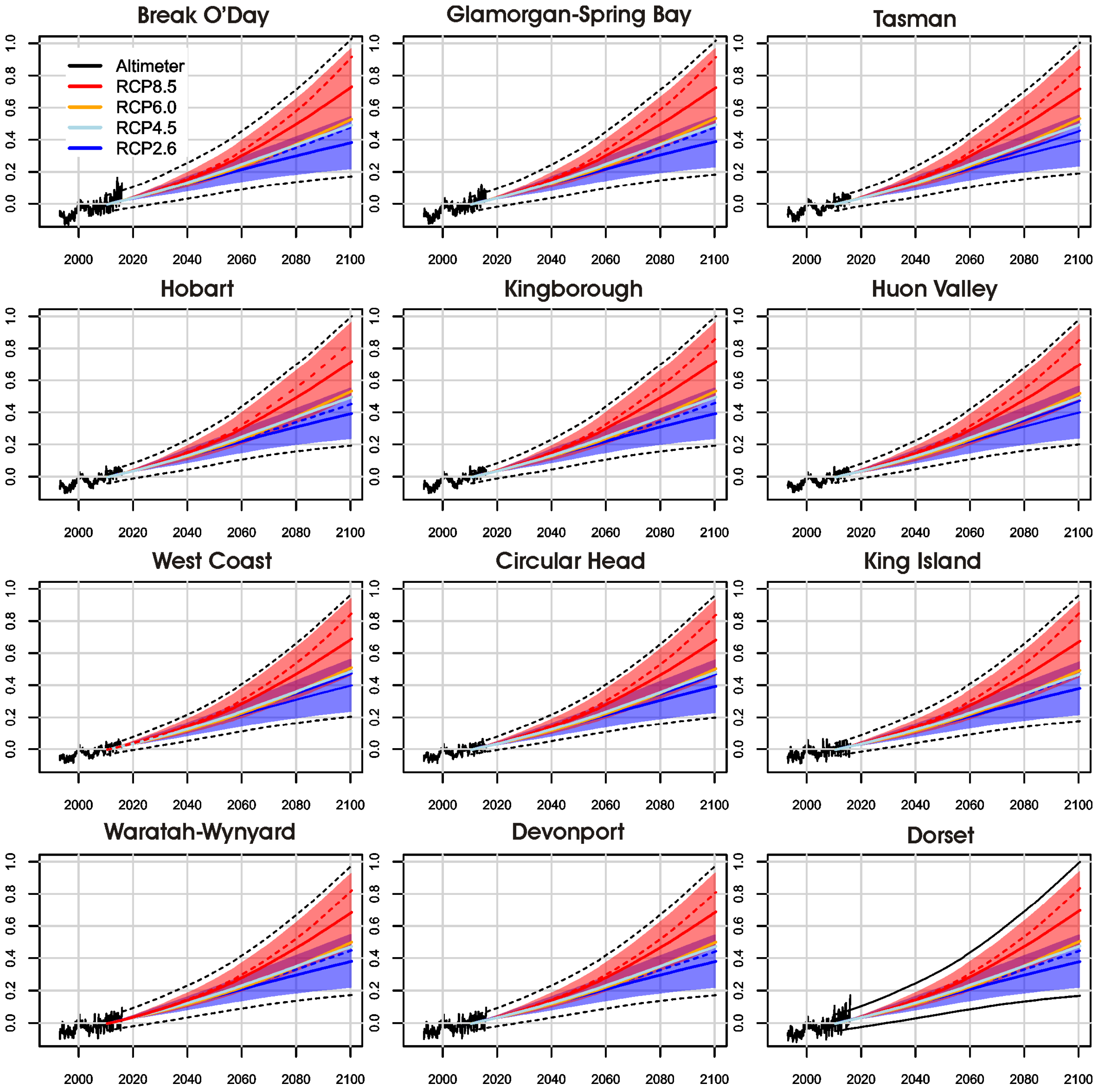

Figure 6. Projected sea-level rise for selected coastal councils. The black line shows the satellite-derived sea-level variability since 1993. Multi-model mean projections (thick red and blue lines) for RCP8.5 and RCP2.6 with the 5-95 percentile range shown by the red and blue shaded regions from 2010 to 2100. The black dashed lines represent estimates of interannual variability determined from the satellite altimeter data combined with the range of the projections. Thick light blue and orange lines represent multi-model mean projections for the RCP 4.5 and 6.0 scenarios, respectively.

4 Extreme Sea-levels and Allowances

The impact of SLR is felt most profoundly during episodes of extreme sea levels. Extreme sea levels can arise from singular oceanic phenomena such as a storm surges but more commonly arise from a combination of natural phenomena that individually may not be extreme. These phenomena occur on a range of time and space scales (Figure 7) in any given coastal location, and thus the contribution of each phenomenon to extreme sea levels varies. Breaking waves occur on the shortest time and space scales in the shoaling zone at the coast. Storm surges affect sea levels on the continental shelf on time scales from hours to several days while climate variability affects sea levels across the ocean basin on interannual time scales. A range of weather conditions cause storm surges and high waves including tropical cyclones and cold fronts. Sea-level extremes are also affected by coastal bathymetry and coastal alignment with respect to the weather conditions.

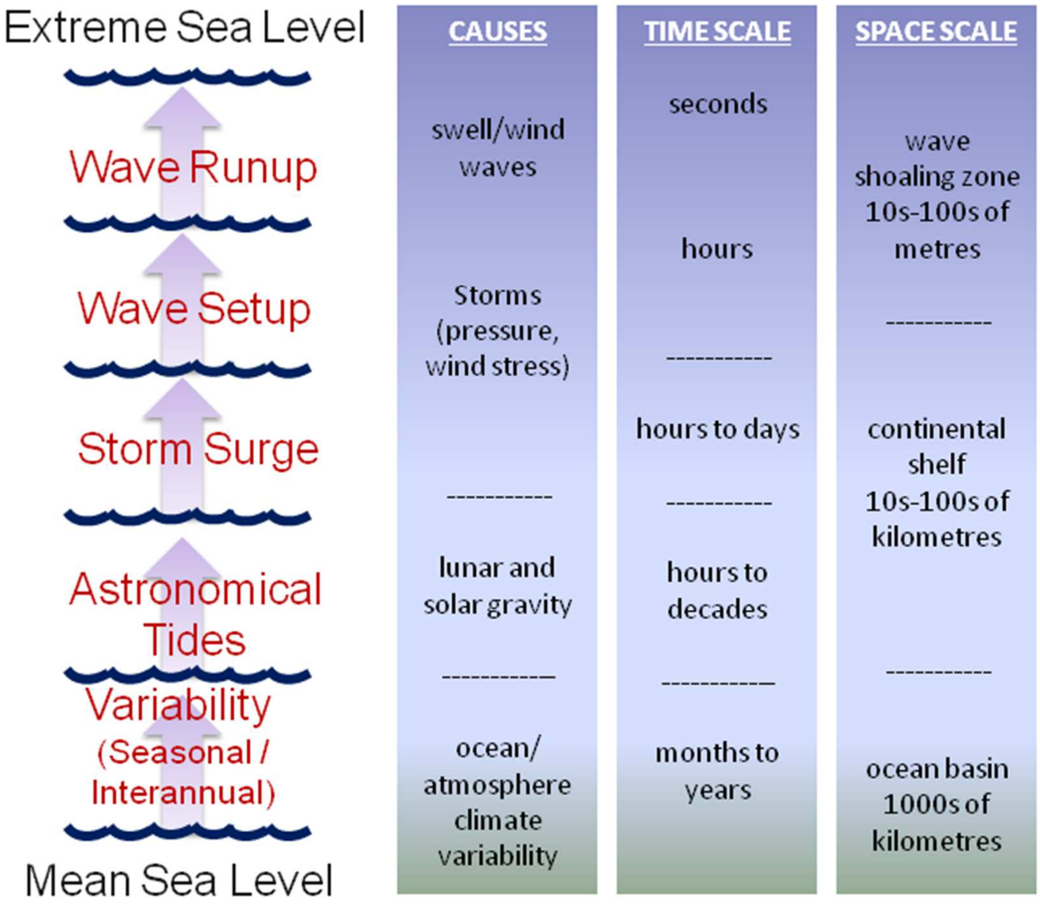

Figure 7. Oceanic phenomena that contribute to total coastal water levels during an extreme sea-level event, their causes and the time and space scales over which they occur (source: McInnes et al, 2016).

While historically, the primary source of extreme sea-level likelihoods has been a statistical analysis of extreme sea levels measured by tide gauges, increasingly hydrodynamic models are used to provide information on water level variations at the coast due to tides and weather forcing. This is because these models provide spatially coherent information covering the entire coastline rather than just the location of the tide gauges.

It should be noted that tide gauges typically do not measure the contributions to extreme sea levels arising from wave breaking because they are typically deployed in sheltered locations such as harbours that are protected from wave breaking. Hydrodynamic models can represent the storm surge and astronomical tide contributions (referred to in combination as storm tides) and although they can also represent wave setup, this requires their coupling to a wave model, high spatial resolution near the coast to resolve the wave breaking zone and detailed bathymetric data. However, the computational requirements of running high resolution wave models and the lack of high resolution bathymetric data in many locations usually precludes such detailed assessments.

The common use of barotropic depth-averaged hydrodynamic models in storm tide assessments means that sea-level variations arising from temperature changes that may occur on seasonal to interannual time scales are not captured, although these effects are small for many parts of the Australian coastline including Tasmania (Haigh et al, 2014). For coastal engineering, planning and adaptation, the likelihoods of extreme sea levels, expressed in terms of return periods (i.e. the average time interval between events that exceed a particular height) or exceedance probabilities (the probability that an event exceeding a particular magnitude will occur in any given year) are of considerable importance in informing the design of built infrastructure and coastal protection. The statistical relationships that are represented in the return period curves (see for example lower panels in Figure 8) also describe the probabilities that an exceedance event will occur in a given year.

In consideration of planning for future sea-level rise and its associated uncertainty, Hunter (2012) proposed an objective method to calculate an allowance from a projected future sea-level range, that if added to current design values would mean that the expected number of exceedances at the future time with sea-level rise would be the same as expected under current day conditions without the sea-level rise. In other words the performance of the mitigation measures would be as effective in the future as they are today.

The mathematical derivation of the allowance is provided in different forms in Hunter (2012), Hunter et al., (2013) and also in McInnes et al., (2015). The form of the allowance used here is given by

$$A = \Delta z + \sigma^2/2\lambda \qquad (1)$$

where Δz is the mean sea-level rise for a given scenario and future time period, σ^2 is derived from the 5-95% confidence limits on the sea-level rise projections and λ is a parameter that describes the slope of the extreme sea-level return period curves (as shown in the bottom panel of Figure 8). Allowances for Tasmania have been calculated based on the sea-level rise projections presented here and scale parameters generated by the study of Haigh et al., (2014) in which a hydrodynamic model was used to simulate sea levels due to tides and storm surges and then statistically analysed to produce return periods.

As indicated in Equation (1), the allowance depends not only on the mean sea-level rise and its uncertainty, but also on the variability of the extreme sea levels, which is represented by λ, the slope of the return period curve. Figure 8 illustrates the relationship between extreme sea-level variability and return periods for two different coastal locations under present conditions. Location A represents a location with large variability in extreme sea levels due to large variations in tidal range between the fortnightly neap and spring cycles and the tendency for large storm surges to occur while location B represents a location with little variation in maximum tides throughout the month and a tendency for smaller storm surges when storms occur. In terms of return periods for storm tides (the combination of the storm surge and astronomical tide) the location on the left is characterised by a steeper return period curve compared to the right (bottom panels).

For the protection of built assets, it is customary to consider the heights associated with particular return periods (e.g. the height of the 1-in-50 or the 1-in-100 year event). These planning benchmarks are illustrated in Figure 8 for present climate conditions. Under a constant sea-level rise these benchmarks will be breached far more frequently in location B compared to location A due to the nature of extreme sea-level variability (Figure 8 middle panel) and this is reflected by a more dramatic shortening of the time interval between exceedance events on the return period curves (Figure 8 lower panel). The change in the frequency of the extremes in location A due to SLR is large in location B compared to A. Therefore, allowances for location B will need to be slightly higher than location A to ensure the frequency of exceedance of extreme sea levels is unchanged from present day levels. This modulation of the allowances is achieved by the term λ in the denominator of the Equation (1).

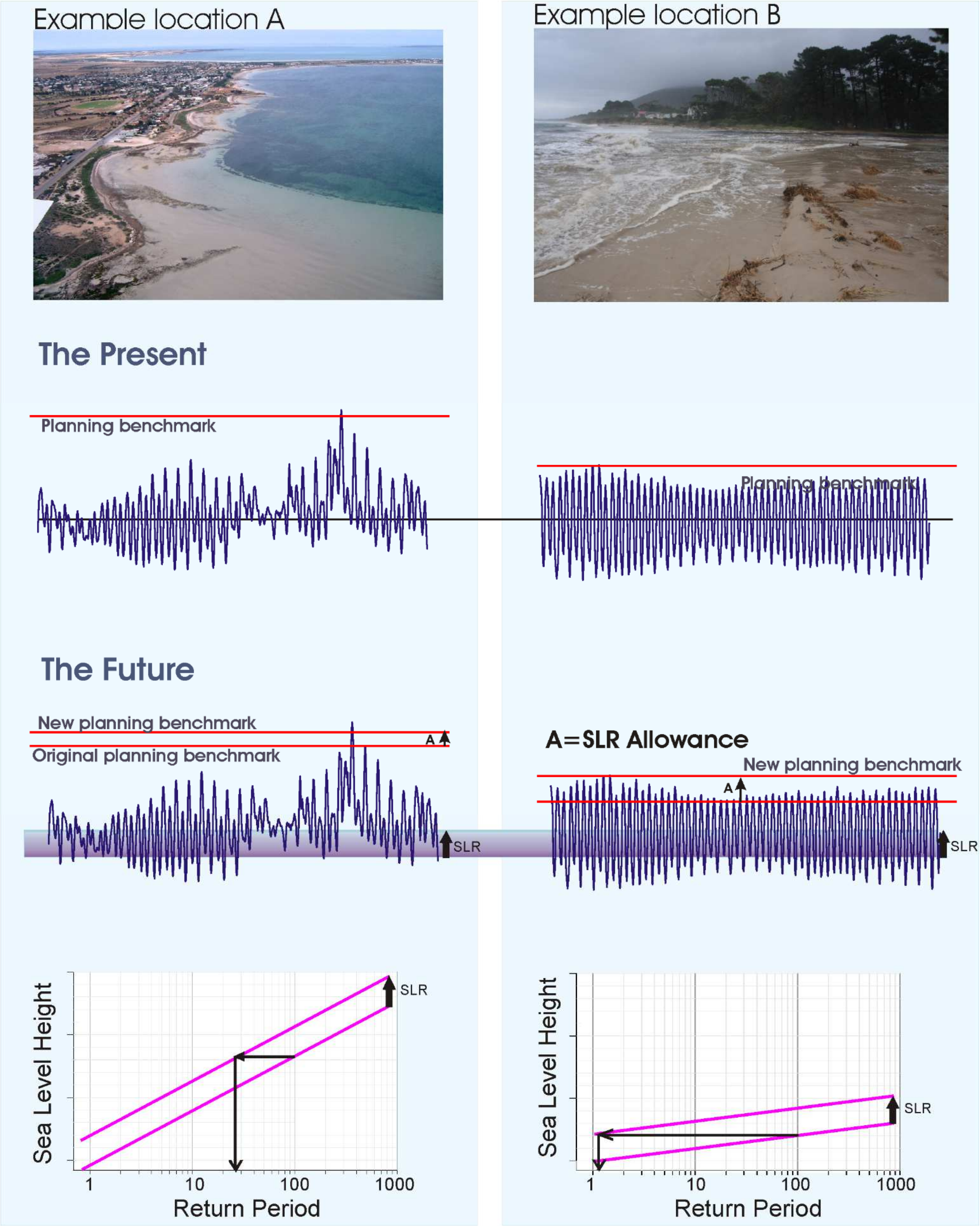

Figure 8. The figure illustrates how different properties of extreme sea levels influence the sea-level allowances developed by Hunter (2012) and Hunter et al (2013). See text for more explanation.

Figure 9 presents allowances for 2100 (relative to 2010) under RCPs 4.5 and 8.5. Allowances are also provided for the coastal councils of Tasmania in Table 2 for 2050 and 2100 for the four RCPs. These allowances show that when the uncertainty on sea-level rise projections is small, as is the case for 2050, the allowances are closer to the median of the sea-level rise range. However as the uncertainty becomes larger, as is the case for 2100, the allowances become larger and tend to lie between the median and 95th percentile sea-level rise projection.

The state-wide average values are also provided in Table 2 and can be compared with values generated previously (Tasmanian Climate Change Office, 2012) for previous coastal inundation mapping (Lacey et al, 2015). For those values, sea-level rise projections were based on the high-end SRES A1FI scenario and yielded planning allowances of 0.2 m for 2050 and 0.8 m for 2100 relative to 2010 values. In the most recent IPCC assessment, RCP 8.5 most closely resembles A1FI in terms of CO_2-equivalent concentrations. The allowances generated using the updated regional SLR scenarios for RCP 8.5 are 0.23 m for 2050 and 0.85 m for 2100 relative to 2010 values indicating a slight increase on the values previously used.

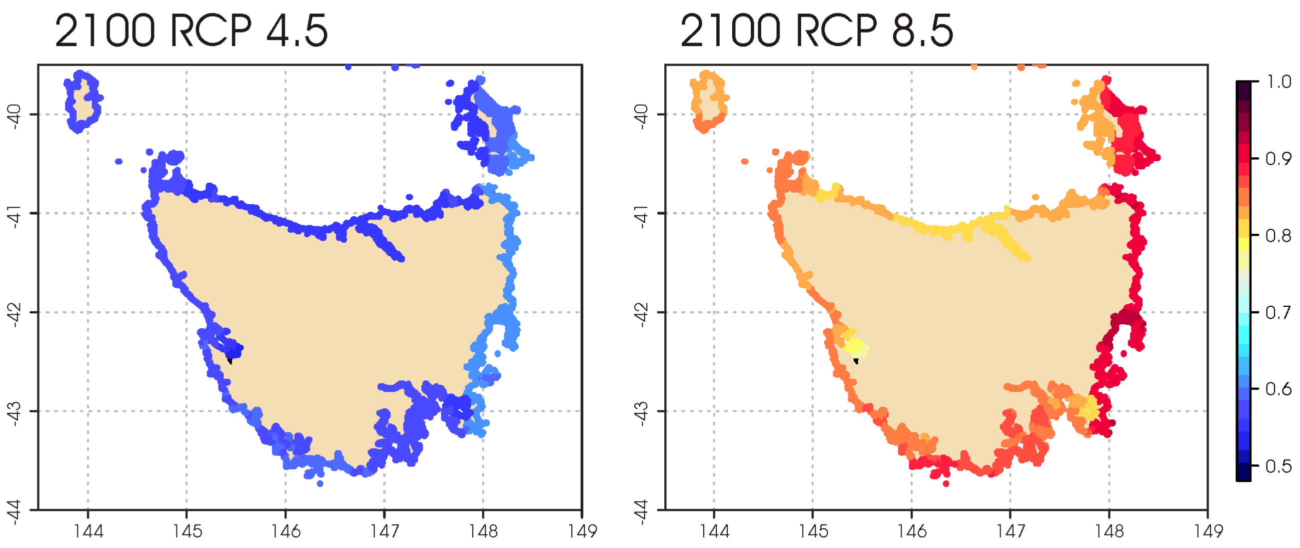

Figure 9. Allowances representing the vertical distance that an asset needs to be raised under a rising sea level so that the present likelihood of flooding does not increase. Values are shown for 2100 and RCPs 4.5 and 8.5. Units are m.

The sea-level rise scenarios and allowances provided in this manual may be used to support council activities around planning and adaptation to ongoing sea-level rise. In relation to the use of allowances, Hunter et al (2013) also noted that “The allowances represent a practical solution to planning for sea-level rise while preserving an acceptable level of inundation likelihood, in cases where ‘getting the allowance wrong’ is manageable. However, in cases where the consequence of inundation would be ‘dire’ (in the sense that the consequence of inundation would be unbearable, no matter how low the likelihood, as in case of the Netherlands), a precautionary approach would be not to use the allowances presented here, but to base an allowance on the best estimate of the *maximum* possible rise”.

This point is important in the context of the allowances provided here, which are based on the 5-95 percentile SLR range. McInnes et al, (2015) notes that the 5-95% range of the model projections, as reported in Church et al., (2013b) is assessed as being ‘likely’ in IPCC terminology. In other words it is assessed that there is only 66.7% probability that future sea-level rise will lie within the range. This ‘*likely*’ assessment of confidence is because of the incomplete knowledge about the future contribution of some components of sea-level rise, particularly relating to the contribution from the ice sheets. This implies a broader range of uncertainty is associated with the sea-level rise projections. A higher range of uncertainty would lead to higher associated allowances.

In considering an appropriate value for the ‘maximum possible’ rise, one could consider the upper (i.e. 95th percentile value) associated with the largest greenhouse gas scenario of the sea-level projections presented here. However, if the consequences of sea levels exceeding the maximum projected range are dire, coastal managers may wish to consider an even higher value of SLR. This may include contributions to SLR that have been omitted from SLR projections because the underpinning scientific understanding of these processes remains uncertain. This was discussed in section 3.1 in relation to the global-averaged sea-level projections reported in the most recent IPCC assessment (Church et al, 2013a). The likely sea-level ranges (analogous to the 5-95 percentile ranges reported here for Australia) did not include an additional contribution from the potential instability of the marine-based sectors of the Antarctic Ice Sheet, because of insufficient scientific evidence to assign likelihoods to this process occurring. In the IPCC Assessment, this process was assessed to not add more than several tenths of a metre of SLR by 2100 above the likely range (Church et al, 2013a). Coastal managers desiring a more conservative projection of SLR may elect to add such as estimate to the upper end of the projected ranges provided here.

Improving our understanding of how ice-sheets may contribute to SLR is an active area of research. As discussed in section 3.1 a number of recent studies generally support the range of SLR reported in Church et al., (2013a). However, some studies that include additional processes such as the collapse of Antarctic ice shelves due to surface melting and hydrofracturing indicate that rises of more than several tenths of a meter by 2100 could occur. This points to a need to continue to assess and revise if necessary the sea-level projections and guidance material provided here.

Table 1 Summary of projected level rise with the 5 to 95 percentile range and allowances (m) for 2050 and 2100 and the sea-level trends over 2080-2100 (mm/yr) for RCPs 2.6, 4.5, 6.0 and 8.5.

BREAK O DAY					
	2050	A	2100	A	Trend 2080 - 2100
rcp26	0.17 [0.11 - 0.24]	0.19	0.39 [0.22 - 0.55]	0.49	4.0 [1.7 - 6.3]
rcp45	0.19 [0.13 - 0.26]	0.21	0.50 [0.32 - 0.68]	0.61	6.0 [3.4 - 8.6]
rcp60	0.18 [0.12 - 0.25]	0.20	0.53 [0.34 - 0.73]	0.66	7.6 [4.7 - 10.7]
rcp85	0.23 [0.16 - 0.30]	0.24	0.73 [0.52 - 0.97]	0.92	11.5 [8.0 - 15.7]
BRIGHTON					
	2050	A	2100	A	Trend 2080 - 2100
rcp26	0.18 [0.12 - 0.24]	0.19	0.40 [0.24 - 0.56]	0.46	4.1 [1.8 - 6.4]
rcp45	0.19 [0.13 - 0.26]	0.20	0.50 [0.33 - 0.68]	0.57	6.1 [3.5 - 8.6]
rcp60	0.18 [0.12 - 0.25]	0.19	0.54 [0.34 - 0.74]	0.63	7.8 [4.8 - 10.9]
rcp85	0.22 [0.15 - 0.30]	0.23	0.72 [0.50 - 0.97]	0.85	11.2 [7.9 - 15.1]
BURNIE					
	2050	A	2100	A	Trend 2080 - 2100
rcp26	0.17 [0.11 - 0.23]	0.18	0.38 [0.22 - 0.55]	0.45	4.1 [1.7 - 6.5]
rcp45	0.18 [0.12 - 0.24]	0.19	0.48 [0.30 - 0.66]	0.55	6.0 [3.3 - 8.7]
rcp60	0.17 [0.11 - 0.23]	0.18	0.50 [0.32 - 0.69]	0.58	7.4 [4.6 - 10.3]
rcp85	0.21 [0.15 - 0.28]	0.22	0.69 [0.46 - 0.93]	0.82	10.9 [7.1 - 15.4]
CENTRAL COAST					
	2050	A	2100	A	Trend 2080 - 2100
rcp26	0.17 [0.11 - 0.23]	0.18	0.38 [0.22 - 0.55]	0.45	4.1 [1.7 - 6.4]
rcp45	0.18 [0.12 - 0.24]	0.19	0.48 [0.30 - 0.66]	0.55	6.0 [3.3 - 8.7]
rcp60	0.17 [0.11 - 0.23]	0.18	0.50 [0.32 - 0.69]	0.58	7.4 [4.6 - 10.3]
rcp85	0.21 [0.15 - 0.28]	0.22	0.69 [0.47 - 0.94]	0.82	10.9 [7.2 - 15.3]
CIRCULAR HEAD					
	2050	A	2100	A	Trend 2080 - 2100
rcp26	0.17 [0.11 - 0.23]	0.18	0.40 [0.23 - 0.57]	0.47	4.3 [1.9 - 6.6]
rcp45	0.18 [0.13 - 0.24]	0.19	0.48 [0.31 - 0.67]	0.57	6.1 [3.4 - 8.8]
rcp60	0.17 [0.11 - 0.24]	0.18	0.51 [0.32 - 0.70]	0.60	7.4 [4.5 - 10.4]
rcp85	0.21 [0.14 - 0.28]	0.22	0.68 [0.46 - 0.94]	0.84	10.8 [6.9 - 15.3]
CLARENCE					
	2050	A	2100	A	Trend 2080 - 2100

rcp26	0.18 [0.12 - 0.24]	0.19	0.40 [0.24 - 0.56]	0.46	4.1 [1.8 - 6.4]
rcp45	0.19 [0.13 - 0.26]	0.20	0.50 [0.33 - 0.68]	0.57	6.1 [3.5 - 8.6]
rcp60	0.18 [0.12 - 0.25]	0.19	0.54 [0.34 - 0.74]	0.63	7.8 [4.8 - 10.9]
rcp85	0.22 [0.15 - 0.30]	0.23	0.72 [0.50 - 0.97]	0.85	11.2 [7.9 - 15.1]
DERWENT VALLEY					
	2050	A	2100	A	Trend 2080 - 2100
rcp26	0.18 [0.12 - 0.24]	0.19	0.40 [0.24 - 0.56]	0.46	4.2 [1.8 - 6.4]
rcp45	0.20 [0.14 - 0.26]	0.20	0.50 [0.33 - 0.68]	0.57	6.1 [3.5 - 8.7]
rcp60	0.18 [0.12 - 0.25]	0.19	0.54 [0.34 - 0.74]	0.63	7.8 [4.9 - 11.0]
rcp85	0.22 [0.15 - 0.30]	0.24	0.73 [0.50 - 0.98]	0.86	11.3 [7.9 - 15.3]
DEVONPORT					
	2050	A	2100	A	Trend 2080 - 2100
rcp26	0.17 [0.11 - 0.23]	0.18	0.38 [0.22 - 0.55]	0.45	4.1 [1.7 - 6.4]
rcp45	0.18 [0.12 - 0.24]	0.19	0.48 [0.30 - 0.66]	0.55	6.0 [3.3 - 8.7]
rcp60	0.17 [0.11 - 0.23]	0.18	0.50 [0.32 - 0.69]	0.58	7.4 [4.6 - 10.3]
rcp85	0.21 [0.15 - 0.28]	0.22	0.69 [0.47 - 0.94]	0.81	10.9 [7.2 - 15.3]
DORSET					
	2050	A	2100	A	Trend 2080 - 2100
rcp26	0.17 [0.11 - 0.23]	0.18	0.38 [0.22 - 0.55]	0.45	4.1 [1.7 - 6.4]
rcp45	0.18 [0.13 - 0.24]	0.19	0.48 [0.30 - 0.66]	0.56	6.0 [3.3 - 8.7]
rcp60	0.17 [0.11 - 0.24]	0.18	0.51 [0.32 - 0.70]	0.60	7.4 [4.6 - 10.4]
rcp85	0.21 [0.15 - 0.28]	0.22	0.70 [0.48 - 0.95]	0.84	11.0 [7.4 - 15.3]
FLINDERS					
	2050	A	2100	A	Trend 2080 - 2100
rcp26	0.17 [0.11 - 0.23]	0.18	0.38 [0.21 - 0.55]	0.49	4.0 [1.7 - 6.3]
rcp45	0.18 [0.13 - 0.24]	0.20	0.48 [0.30 - 0.66]	0.61	5.9 [3.3 - 8.6]
rcp60	0.18 [0.11 - 0.24]	0.19	0.51 [0.32 - 0.70]	0.65	7.4 [4.5 - 10.4]
rcp85	0.21 [0.15 - 0.28]	0.23	0.70 [0.48 - 0.95]	0.92	11.1 [7.5 - 15.4]
GEORGE TOWN					
	2050	A	2100	A	Trend 2080 - 2100
rcp26	0.17 [0.11 - 0.23]	0.18	0.38 [0.22 - 0.55]	0.44	4.1 [1.7 - 6.4]
rcp45	0.18 [0.12 - 0.24]	0.19	0.48 [0.30 - 0.66]	0.55	5.9 [3.3 - 8.6]
rcp60	0.17 [0.11 - 0.24]	0.18	0.50 [0.32 - 0.70]	0.59	7.3 [4.5 - 10.3]
rcp85	0.21 [0.15 - 0.28]	0.22	0.69 [0.47 - 0.94]	0.82	11.0 [7.3 - 15.3]
GLAMORGAN SPRING BAY					
	2050	A	2100	A	Trend 2080 - 2100
rcp26	0.18 [0.12 - 0.24]	0.19	0.39 [0.23 - 0.56]	0.49	4.1 [1.8 - 6.3]
rcp45	0.20 [0.13 - 0.26]	0.21	0.50 [0.33 - 0.68]	0.61	6.1 [3.5 - 8.6]
rcp60	0.19 [0.12 - 0.25]	0.20	0.54 [0.34 - 0.74]	0.68	7.8 [4.9 - 10.9]
rcp85	0.23 [0.16 - 0.30]	0.24	0.73 [0.51 - 0.97]	0.92	11.3 [8.0 - 15.2]
GLENORCHY					
	2050	A	2100	A	Trend 2080 - 2100
rcp26	0.18 [0.12 - 0.24]	0.19	0.40 [0.24 - 0.56]	0.46	4.1 [1.8 - 6.4]
rcp45	0.19 [0.13 - 0.26]	0.20	0.50 [0.33 - 0.68]	0.57	6.1 [3.5 - 8.6]
rcp60	0.18 [0.12 - 0.25]	0.19	0.54 [0.34 - 0.74]	0.63	7.8 [4.8 - 10.9]
rcp85	0.22 [0.15 - 0.30]	0.23	0.72 [0.50 - 0.97]	0.85	11.2 [7.9 - 15.1]

HOBART					
	2050	A	2100	A	Trend 2080 - 2100
rcp26	0.18 [0.12 - 0.24]	0.19	0.40 [0.24 - 0.56]	0.46	4.1 [1.8 - 6.4]
rcp45	0.19 [0.13 - 0.26]	0.20	0.50 [0.33 - 0.68]	0.57	6.1 [3.5 - 8.6]
rcp60	0.18 [0.12 - 0.25]	0.19	0.54 [0.34 - 0.74]	0.63	7.8 [4.8 - 10.9]
rcp85	0.22 [0.15 - 0.30]	0.23	0.72 [0.50 - 0.97]	0.85	11.2 [7.9 - 15.1]
HUON VALLEY					
	2050	A	2100	A	Trend 2080 - 2100
rcp26	0.18 [0.12 - 0.24]	0.19	0.40 [0.24 - 0.57]	0.48	4.3 [1.9 - 6.6]
rcp45	0.19 [0.13 - 0.25]	0.20	0.50 [0.32 - 0.68]	0.58	6.2 [3.5 - 8.8]
rcp60	0.18 [0.12 - 0.24]	0.19	0.52 [0.34 - 0.72]	0.62	7.6 [4.7 - 10.7]
rcp85	0.22 [0.15 - 0.29]	0.23	0.70 [0.47 - 0.96]	0.86	11.0 [7.3 - 15.3]
KING ISLAND					
	2050	A	2100	A	Trend 2080 - 2100
rcp26	0.17 [0.11 - 0.23]	0.18	0.38 [0.22 - 0.55]	0.47	4.2 [1.7 - 6.5]
rcp45	0.18 [0.12 - 0.24]	0.19	0.47 [0.29 - 0.66]	0.58	6.0 [3.3 - 8.7]
rcp60	0.17 [0.11 - 0.23]	0.18	0.50 [0.31 - 0.69]	0.61	7.2 [4.4 - 10.3]
rcp85	0.21 [0.14 - 0.28]	0.22	0.68 [0.45 - 0.93]	0.86	10.8 [7.0 - 15.3]
KINGBOROUGH					
	2050	A	2100	A	Trend 2080 - 2100
rcp26	0.18 [0.12 - 0.24]	0.19	0.40 [0.24 - 0.56]	0.47	4.1 [1.8 - 6.4]
rcp45	0.19 [0.13 - 0.26]	0.20	0.50 [0.33 - 0.68]	0.58	6.1 [3.5 - 8.6]
rcp60	0.18 [0.12 - 0.25]	0.20	0.54 [0.34 - 0.74]	0.64	7.8 [4.8 - 10.9]
rcp85	0.22 [0.15 - 0.30]	0.24	0.72 [0.50 - 0.97]	0.87	11.2 [7.9 - 15.1]
LATROBE					
	2050	A	2100	A	Trend 2080 - 2100
rcp26	0.17 [0.11 - 0.23]	0.18	0.38 [0.22 - 0.55]	0.44	4.1 [1.7 - 6.4]
rcp45	0.18 [0.12 - 0.24]	0.19	0.48 [0.30 - 0.66]	0.55	5.9 [3.3 - 8.6]
rcp60	0.17 [0.11 - 0.24]	0.18	0.50 [0.32 - 0.70]	0.58	7.3 [4.5 - 10.3]
rcp85	0.21 [0.15 - 0.28]	0.22	0.69 [0.47 - 0.94]	0.82	11.0 [7.3 - 15.3]
LAUNCESTON					
	2050	A	2100	A	Trend 2080 - 2100
rcp26	0.17 [0.11 - 0.23]	0.18	0.38 [0.22 - 0.55]	0.45	4.1 [1.7 - 6.4]
rcp45	0.18 [0.13 - 0.24]	0.19	0.48 [0.30 - 0.66]	0.55	6.0 [3.3 - 8.7]
rcp60	0.17 [0.11 - 0.24]	0.18	0.51 [0.32 - 0.70]	0.59	7.4 [4.6 - 10.4]
rcp85	0.21 [0.15 - 0.28]	0.22	0.70 [0.48 - 0.95]	0.83	11.0 [7.4 - 15.3]
SORELL					
	2050	A	2100	A	Trend 2080 - 2100
rcp26	0.18 [0.12 - 0.24]	0.19	0.40 [0.24 - 0.56]	0.45	4.1 [1.8 - 6.4]
rcp45	0.19 [0.13 - 0.26]	0.20	0.50 [0.33 - 0.68]	0.57	6.1 [3.5 - 8.6]
rcp60	0.18 [0.12 - 0.25]	0.19	0.54 [0.34 - 0.74]	0.62	7.8 [4.8 - 10.9]
rcp85	0.22 [0.15 - 0.30]	0.23	0.72 [0.50 - 0.97]	0.84	11.2 [7.9 - 15.1]
TASMAN					
	2050	A	2100	A	Trend 2080 - 2100
rcp26	0.18 [0.12 - 0.24]	0.19	0.40 [0.24 - 0.56]	0.46	4.1 [1.8 - 6.4]
rcp45	0.19 [0.13 - 0.26]	0.20	0.50 [0.33 - 0.68]	0.57	6.1 [3.5 - 8.6]

rcp60	0.18 [0.12 - 0.25]	0.19	0.54 [0.34 - 0.74]	0.63	7.8 [4.8 - 10.9]
rcp85	0.22 [0.15 - 0.30]	0.24	0.72 [0.50 - 0.97]	0.86	11.2 [7.9 - 15.1]
WARATAH WYNYARD					
	2050	A	2100	A	Trend 2080 - 2100
rcp26	0.17 [0.11 - 0.23]	0.18	0.38 [0.22 - 0.55]	0.45	4.1 [1.7 - 6.5]
rcp45	0.18 [0.12 - 0.24]	0.19	0.48 [0.30 - 0.66]	0.56	6.0 [3.3 - 8.7]
rcp60	0.17 [0.11 - 0.23]	0.18	0.50 [0.32 - 0.69]	0.59	7.4 [4.6 - 10.3]
rcp85	0.21 [0.15 - 0.28]	0.22	0.69 [0.46 - 0.93]	0.83	10.9 [7.1 - 15.4]
WEST COAST					
	2050	A	2100	A	Trend 2080 - 2100
rcp26	0.17 [0.12 - 0.24]	0.18	0.40 [0.24 - 0.57]	0.48	4.4 [2.0 - 6.7]
rcp45	0.19 [0.13 - 0.25]	0.20	0.49 [0.31 - 0.67]	0.58	6.2 [3.5 - 8.9]
rcp60	0.18 [0.12 - 0.24]	0.19	0.51 [0.33 - 0.71]	0.61	7.5 [4.6 - 10.5]
rcp85	0.21 [0.15 - 0.28]	0.23	0.69 [0.46 - 0.95]	0.85	10.8 [7.0 - 15.3]
WEST TAMAR					
	2050	A	2100	A	Trend 2080 - 2100
rcp26	0.17 [0.11 - 0.23]	0.18	0.38 [0.22 - 0.55]	0.44	4.1 [1.7 - 6.4]
rcp45	0.18 [0.12 - 0.24]	0.19	0.48 [0.30 - 0.66]	0.55	5.9 [3.3 - 8.6]
rcp60	0.17 [0.11 - 0.24]	0.18	0.50 [0.32 - 0.70]	0.58	7.3 [4.5 - 10.3]
rcp85	0.21 [0.15 - 0.28]	0.22	0.69 [0.47 - 0.94]	0.82	11.0 [7.3 - 15.3]
Average of all councils					
	2050	A	2100	A	Trend 2080 - 2100
rcp26	0.17 [0.11-0.24]	0.18	0.39 [0.23-0.56]	0.46	4.13 [1.77-6.43]
rcp45	0.19 [0.13-0.25]	0.20	0.49 [0.31-0.67]	0.57	6.04 [3.40-8.66]
rcp60	0.18 [0.12-0.24]	0.19	0.52 [0.33-0.72]	0.61	7.55 [4.66-10.59]
rcp85	0.22 [0.15-0.29]	0.23	0.70 [0.48-0.95]	0.85	11.07 [7.51-15.27]

5 Summary and Conclusions

This report provides updated sea level rise projections and allowances for Tasmania based on modelling and projections undertaken for the IPCC 5AR and Australia-wide projections reported in McInnes et al (2015). The projections are provided for four Representative Concentration Pathways ranging from a high-end 'business-as-usual' scenario (RCP 8.5) to a strong mitigation scenario (RCP 2.6). For Tasmania as a whole, projections of the median sea-level rise and 5-95% model range in 2050 are 0.17 [0.11-0.24] m and 0.22 [0.15-0.29] m relative to 2100 values under RCP 2.6 and 8.5 respectively. For 2100 the projected increases are 0.22 [0.15-0.29] m and 0.70 [0.48-0.95] m for RCP 2.6 and 8.5 respectively. The projections vary spatially around Tasmania with the largest increases expected on the east coast of Tasmania and the smallest on the west coast.

Allowances, which provide estimates of how much present planning heights would need to be raised under uncertain sea-level rise to ensure that the expected frequency of future exceedances remains the same as in the present climate, have also been updated for Tasmania. The revised allowances in 2050 are 0.18 m and 0.23 m for RCPs 2.6 and 8.5 respectively while in 2100 they are 0.46 m and 0.85 m respectively. The allowances previously calculated for Tasmania were 0.2 m in 2050 and 0.8m in 2100 relative to 2010 based on a high-end emission scenario (SRES A1FI) from the IPCC AR4 (IPCC, 2007), the most similar in the current scenarios being RCP8.5. The revised allowances are similar but slightly higher than those previously calculated, the differences arising from the revised sea level projections and their ranges together with a different extreme sea level data set used to underpin the allowance calculations based on McInnes et al (2012b). The allowances also exhibit variation around the Tasmanian coast with the highest allowances (of around 0.92 m) calculated for the northeast coast and the lowest values (of around 0.82 m) calculated for the central north coast.

The projections and allowances provided here build on progress in understanding and developing projections of sea-level change over the last decade as summarised in the IPCC AR5 (Church et al., 2013a) and recent studies attributing ocean thermal expansion (Slangen et al., 2014), glacier mass loss (Marzeion et al., 2014) and total sea-level rise (Slangen et al. 2016) to anthropogenic factors. Despite this progress, the largest uncertainty remains in the contribution of the Antarctic Ice Sheet to future sea-level rise with recent observations (Rignot et al., 2014) indicating increased loss of ice from West Antarctica. Recent modelling (Favier et al., 2014; Joughin et al., 2014; Cornford et al. 2015; Ritz et al. 2015) has been able to simulate the increased flow of individual glaciers and the projections of mass loss in these studies are consistent with the Antarctic contribution used in the IPCC AR5 and here. Nevertheless, understanding of the relevant ocean-ice sheet processes (Alley and Joughin, 2012; Willis and Church, 2012) are still incomplete and the possibility of higher rates of sea-level rise cannot be excluded (Church et al., 2013a, DeConto and Pollard, 2016).

Regional projections of sea-level rise depend on many factors. During the 20th century, Australian rates of relative sea-level rise were below the estimated global average rise because of upward relative land motion from GIA. This process will continue during the 21st century but will become relatively less important as other contributions increase, particularly larger contributions from glaciers and ice sheets leading to a larger than global-averaged rise in the Australian region for larger ice sheet contributions.

Variability in sea-level from decadal and interannual climate variability will continue into the future, resulting in times when the sea level and the rates of rise will be measurably above or below the global-averaged and regional sea-level projections presented here. Observed sea levels and rates of rise off north and west coasts of Australia are currently above the projections as a result of this variability. This variability will continue to confound evaluation of regional climate change projections. However, estimates are that the local climate change sea-level signal, compared to the average over 1986 to 2005, will begin to emerge from this natural variability by 2030 off the east coast of Australia and 2040 off the west coast (Lyu et al., 2014) stressing the urgency for future planning and risk management to take account of the combined impact of the sea-level rise and natural variability signals. Seasonal sea-level predictions (up to nine months in advance) (Miles et al., 2014; McIntosh et al. 2015) may be a useful tool in helping to manage these risks.

Any change in the El Nino Southern Oscillation or other modes of variability have the potential to impact Australian sea levels. However, the regional pattern of dynamic ocean sea-level change remains inadequately understood. Further studies of interannual and decadal variability, and detection and attribution of sea-level variability and change are a priority to address these issues.

It is important to note that sea-level rise around Australia will continue beyond 2100 in all of the scenarios considered. For the RCP8.5 scenario, the rates of sea-level rise by the end of the 21st century, will be well above the 20th century rate and approaching average rates (1 m/century for many millennia) experienced during the last deglaciation of the Earth from 22 thousand to 6 thousand years ago.

The expected frequency of exceedance of sea levels associated with particular ARIs provide relevant context for planning for and adapting to future sea-level rise. Therefore, allowances have been calculated that provide estimates of how much present planning heights would need to be raised under uncertain sea-level rise to ensure that the expected frequency of future exceedances remains the same as in the present climate. It should be noted that the allowances are based on present climate extreme sea-level behaviour and do not take into account future changes in weather conditions that could change future extreme sea levels. To date there are few studies of future changes in extreme sea levels around the Australian coast, but those completed suggest that the influence of climate change on the 1-in-100 year storm tide may be much smaller than the projected MSL change and therefore neglected to first order for most locations (see McInnes et al; 2015, 2016 for more discussion), however, more investigation is needed to better understand changes in extreme sea levels at the regional scale. Values vary around the Tasmanian coast depending on the regional variations in sea-level rise, together with its uncertainty and characteristics of tides and storm surges. Moderate confidence is given to the allowance values provided because their calculation has utilised modelled extreme sea-level data, which contains uncertainties and also because the uncertainty associated with future sea-level rise may be larger than expressed by the 5 to 95% model range.

The large uncertainty in sea-level projections towards the end of the Century compared to those for 2030 implies that flexible strategies are needed for adaptation. The ‘adaptation pathways’ approach affords this flexibility by characterising different adaptation strategies in terms of adaptation tipping points. This approach favours flexible and reversible options and the delay of decisions to maximise future options for adaptation. It also allows the adaptation strategies to be assessed and revised if necessary as understanding of the processes contributing to SLR improve, particularly those processes related to uncertainties in the future contribution of the Antarctic ice sheet.

References

Alley R.B. and Joughin I. (2012) Modeling Ice-Sheet Flow. Science, 336:551-552.

Boening, C., J. K. Willis, F. W. Landerer, R. S. Nerem, and J. Fasullo (2012) The 2011 La Niña: So strong, the oceans fell, Geophysical Research Letters, 39(19) L19602.

Chao, B. F., Y. H. Wu, and Y. S. Li (2008), Impact of artificial reservoir water impoundment on global sea level, *Science*, *320*(5873), 212-214.

Church J.A., Clark P.U., Cazenave A., Gregory J.M., Jevrejeva S., Levermann A., Merrifield M.A., Milne G.A., Nerem R.S., Nunn P.D., Payne A.J., Pfeffer W.T., Stammer D., Unnikrishnan A.S. (2013a) Sea Level Change., in: T. F. Stocker, et al. (Eds.), In: Climate Change 2013a: The Physical Science Basis. Contribution of Working Group I to the Fifth Assessment Report of the Intergovernmental Panel on Climate Change, Cambridge University Press, Cambridge, United Kingdom and New York, NY, USA.

Church JA, Clark PU, Cazenave A, Gregory JM, Jevrejeva S, Levermann A, M. A. Merrifield, G. A. Milne, R. S. Nerem, P. D. Nunn, A. J. Payne, W. T. Pfeffer, D. Stammer and A. S. Unnikrishnan, (2013b), Sea level change supplementary material, pages 13SM-1–8. In: Stocker TF, Qin D, Plattner G-K, Tignor M, Allen SK, Boschung J, Nauels A, Xia Y, Bex V, Midgley PM, editors. Climate change 2013: the physical science basis. Contribution of Working Group I to the fifth assessment report of the intergovernmental panel on climate change. Cambridge: Cambridge University Press; Cambridge, United Kingdom and New York, NY, USA.

Church, J. A., J. M. Gregory, N. J. White, S. M. Platten, and J. X. Mitrovica (2011a), Understanding and projecting sea level change, *Oceanography*, *24*(2), 130-143.

Church, J. A., N. J. White, L. F. Konikow, C. M. Domingues, J. G. Cogley, E. Rignot, J. M. Gregory, M. R. van den Broeke, A. J. Monaghan, and I. Velicogna (2011b), Revisiting the Earth's sea-level and energy budgets from 1961 to 2008, *Geophys. Res. Lett.*, *38*(18), L18601.

Clark, P. U., J. A. Church, J. M. Gregory, and A. J. Payne (2015) Recent Progress in Understanding and Projecting Regional and Global Mean Sea Level Change, Curr Clim Change Rep, 1(4), 224-246.

Department of Climate Change, (2009) Climate Change Risks to Australia’s Coast. A First Pass National Assessment. Report published by the Department of Climate Change, Australian Government, Canberra, Australia, 172 pp.

Cornford, S. L., et al. (2015) Century-scale simulations of the response of the West Antarctic Ice Sheet to a warming climate, The Cryosphere, 9(4), 1579-1600.

DeConto, R. M., and D. Pollard (2016), Contribution of Antarctica to past and future sea-level rise, *Nature*, *531*(7596), 591-597.

Dieng, H. B., N. Champollion, A. Cazenave, Y. Wada, E. Schrama, and B. Meyssignac (2015) Total land water storage change over 2003–2013 estimated from a global mass budget approach, Environmental Research Letters, 10(12), 124010.

Favier, L., G. Durand, S. L. Cornford, G. H. Gudmundsson, O. Gagliardini, F. Gillet-Chaulet, T. Zwinger, A. J. Payne, and A. M. Le Brocq (2014) Retreat of Pine Island Glacier controlled by marine ice-sheet instability, Nature Clim. Change, 4(2), 117-121

Gregory, J. M., et al. (2012) Twentieth-Century Global-Mean Sea Level Rise: Is the Whole Greater than the Sum of the Parts?, Journal of Climate, *26*(13), 4476-4499.

Haigh I., Wijeratne E.M.S., MacPherson L., Pattiaratchi C., Mason M., Crompton R., and George S. (2014) Estimating present day extreme water level exceedance probabilities around the coastline of Australia: tides, extra - tropical storm surges and mean sea level. Climate Dynamics, 42, 121 - 138.

Hoeke R.K., McInnes K.L., O’Grady J.G. (2015) Wind and wave setup contributions to extreme sea Levels at a tropical high island: A stochastic cyclone simulation study for Apia, Samoa J. Marine Science and Engineering 3:1117 - 1135. DOI: 10.3390/jmse3031117.

Hunter J. (2012) A simple technique for estimating an allowance for uncertain sea-level rise. Climatic Change, 113:239-252. DOI: 10.1007/s10584-011-0332-1.

Hunter J.R., Church J.A., White N.J., Zhang X. (2013) Towards a global regionally varying allowance for sea-level rise. Ocean Engineering, 1-11. DOI: 10.1016/j.oceaneng.2012.12.041i.

IPCC, (2007) Summary for Policymakers. In: Climate Change 2007: The Physical Science Basis. Contribution of Working Group I to the Fourth Assessment Report of the Intergovernmental Panel on Climate Change [Solomon, S., D. Qin, M. Manning, Z. Chen, M. Marquis, K.B. Averyt, M. Tignor and H.L. Miller (eds.)]. Cambridge University Press, Cambridge, UK, pp. 1-18.

Joughin I., Smith B.E., Medley B. (2014) Marine Ice Sheet Collapse Potentially Under Way for the Thwaites Glacier Basin, West Antarctica. Science, 344:735-738. DOI: 10.1126/science.1249055.

Kendall R.A., Mitrovica J.X., Milne G.A. (2005) On post-glacial sea level - II. Numerical formulation and comparative results on spherically symmetric models. Geophysical Journal International, 161:679-706. DOI: 10.1111/j.1365-246X.2005.02553.x.

Kjeldsen, K. K., et al. (2015) Spatial and temporal distribution of mass loss from the Greenland Ice Sheet since AD 1900, Nature, 528(7582), 396-400.

Konikow, L. F. (2011), Contribution of global groundwater depletion since 1900 to sea-level rise, *Geophys. Res. Lett.*, *38*(17), L17401.

Lacey M., Hunter J., and Mount R., 2015 Coastal Inundation Mapping for Tasmania - Stage 3. Report for Department of Premier and Cabinet. January 2015. 48pp.

Levermann, A., et al. (2014) Projecting Antarctic ice discharge using response functions from SeaRISE ice-sheet models, Earth Syst. Dynamics, 5(2), 271-293.

Lorbacher, K., S. J. Marsland, J. A. Church, S. M. Griffies, and D. Stammer (2012) Rapid barotropic sea level rise from ice sheet melting, J. Geophys. Res., *117*(C6), C06003.2

Lyu, K., and X. Zhang, J.A. Church, A.B.A. Slangen and J. Hu (2014) Time of emergence for regional sea-level change. Nature Climate Change, 4, 1006-1010 doi: 10.1038/nclimate2397.

Marcos, M., and A. Amores (2014), Quantifying anthropogenic and natural contributions to thermosteric sea level rise, Geophysical Research Letters, *41*(7), 2502-2507.

Marzeion B., Cogley J.G., Richter K., Parkes D. (2014) Attribution of global glacier mass loss to anthropogenic and natural causes. Science 345:919-921.

McInnes, K.L., Lipkin, F., O'Grady, J.G. and Inman, M. 2012a: Modelling and Mapping of Coastal Inundation under Future Sea Level. A report for Sydney Coastal Councils Group, 62pp.

McInnes, K.L., Church, J.A., Monselesan, D. Hunter, J.R. O'Grady, J.G., Haigh, I.D. and Zhang, X., (2015) Sea-level Rise Projections for Australia: Information for Impact and Adaptation Planning. Australian Meteorology and Oceanography Journal. 65: 127–149.

McInnes, K.L., O'Grady, J.G. Hemer, M, Macadam, I., Abbs, D.J., White, C.J., Corney, S.P., Grose, M.R., Holz, G.K., Gaynor, S.M. and Bindoff, N.L. 2012b: Extreme Tide and Sea - Level Events. Climate Futures for Tasmania Technical Report. Antarctic Climate and Ecosystems CRC. 40 pp.

McInnes, K.L., Macadam, I., Hubbert, G.D. and O'Grady, J.G. (2013) An assessment of current and future vulnerability to coastal inundation due to sea level extremes in Victoria, southeast Australia Int. J.: Clim. 33: 33 - 47. DOI: 10.1002/joc.3405

McInnes, K.L., White, C.J., Haigh, I.D., Hemer, M.A., Hoeke, R.K., Holbrook, N.J., Kiem, A.S., Oliver, E.C.J., Ranasinghe, R., Walsh, K.J.E., Westra, S. and Cox, R. (2016) Natural hazards in Australia: sea level and coastal extremes. Climatic Change. DOI 10.1007/s10584 - 016 - 1647 - 8.

McIntosh, P. C., J. A. Church, E. R. Miles, K. Ridgway, and C. M. Spillman (2015), Seasonal coastal sea level prediction using a dynamical model, Geophysical Research Letters, *42*(16), 6747-6753.

Miles, E., C. Spillman, J. Church, and P. McIntosh (2014), Seasonal prediction of global sea level anomalies using an ocean–atmosphere dynamical model, *Climate Dynamics*, *43*(7-8), 2131-2145.

Moore J.C., S.Jevrejeva, Grinsted A. (2011) The historical global sea level budget. Annals of Glaciology 52:8-14.

Nakicenovic, N., J. Alcamo, G. Davis, B. de Vries, J. Fenhann, S. Gaffin, K. Gregory, A. Grübler, T.Y. Jung, T. Kram, E.L. La Rovere, L. Michaelis, S. Mori, T. Morita, W. Pepper, H. Pitcher, L. Price, K. Riahi, A. Roehrl, H-H. Rogner, A. Sankovski, M. Schlesinger, P. Shukla, S. Smith, R. Swart, S. van Rooijen, N. Victor, and Z. Dadi, 2000: Special Report on Emissions Scenarios: A Special Report of Working Group III of the Intergovernmental Panel on Climate Change. Cambridge University Press, Cambridge, UK, 599 pp.

Nick, F. M., A. Vieli, M. L. Andersen, I. Joughin, A. Payne, T. L. Edwards, F. Pattyn, and R. S. W. van de Wal (2013), Future sea-level rise from Greenland/'s main outlet glaciers in a warming climate, *Nature*, *497*(7448), 235-238.

Ngo-Duc, T., K. Laval, J. Polcher, A. Lombard, and A. Cazenave (2005), Effects of land water storage on global mean sea level over the past half century, *Geophysical Research Letters*, *32*(9 (May 12)), 9704-9707.

Peltier W.R. (2004) Global Glacial Isostasy and the Surface of the Ice-age Earth. The ICE-5G (VM2) Model and GRACE. Annual Review of Earth and Planetary Sciences 32:111-149.

Reager, J. T., A. S. Gardner, J. S. Famiglietti, D. N. Wiese, A. Eicker, and M.-H. Lo (2016) A decade of sea level rise slowed by climate-driven hydrology, Science, 351(6274), 699-703.

Rignot E., Mouginot J., Morlighem M., Seroussi H., Scheuchl B. (2014) Widespread, rapid grounding line retreat of Pine Island, Thwaites, Smith, and Kohler glaciers, West Antarctica, from 1992 to 2011. Geophysical Research Letters 41:3502-3509. DOI: 10.1002/2014gl060140.

Ritz, C., T. L. Edwards, G. Durand, A. J. Payne, V. Peyaud, and R. C. A. Hindmarsh (2015) Potential sea-level rise from Antarctic ice-sheet instability constrained by observations, Nature, 528(7580), 115-118.

Shepherd A., Ivins E.R., A G., Barletta V.R., Bentley M.J., Bettadpur S., Briggs K.H., Bromwich D.H., Forsberg R., Galin N., Horwath M., Jacobs S., Joughin I., King M.A., Lenaerts J.T.M., Li J., Ligtenberg S.R.M., Luckman A., Luthcke S.B., McMillan M., Meister R., Milne G., Mouginot J., Muir A., Nicolas J.P., Paden J., Payne A.J., Pritchard H., Rignot E., Rott H., Sørensen L.S., Scambos T.A., Scheuchl B., Schrama E.J.O., Smith B., Sundal A.V., van Angelen J.H., van de Berg W.J., van den Broeke M.R., Vaughan D.G., Velicogna I., Wahr J., Whitehouse P.L., Wingham D.J., Yi D., Young D., Zwally H.J. (2012) A Reconciled Estimate of Ice-Sheet Mass Balance. Science 338:1183-1189.

Slangen A.B.A., Church J.A., Zhang X., Monselesan D. (2014) Detection and attribution of global mean thermosteric sea level change. Geophysical Research Letters 41(16), 5951-5959. DOI: 10.1002/2014gl061356.

Slangen A.B.A., Katsman C., van de Wal R., Vermeersen L., Riva R. (2012) Towards regional projections of twenty-first century sea-level change based on IPCC SRES scenarios. Climate Dynamics 38:1191-1209.

Slangen, A. B. A., Church, J. A., Agosta, C., Fettweis, X., Marzeion, B., and Richter, K. (2016), Anthropogenic forcing dominates global mean sea-level rise since 1970, Nature Clim. Change, advance online publication.

Tasmanian Climate Change Office (2012), Derivation of the Tasmanian Sea Level Rise Planning Allowances - Technical Paper. August 2012, 19pp.

Wada Y., van Beek L.P.H., Sperna Weiland F.C., Chao B.F., Wu Y.-H., Bierkens M.F.P. (2012) Past and future contribution of global groundwater depletion to sea-level rise. Geophysical Research Letters, 39:L09402. DOI: 10.1029/2012gl051230.

White N.J., Haigh I.D., Church J.A., Koen T., Watson C.S., Pritchard T.R., Watson P.J., Burgette R.J., McInnes K.L., You Z.-J., Zhang X., Tregoning P. (2014) Australian sea levels—Trends, regional variability and influencing factors. Earth-Science Reviews, 136:155-174. DOI: http://dx.doi.org/10.1016/j.earscirev.2014.05.011.

Willis J.K., Church J.A. (2012) Regional Sea-Level Projection. Science, 336:550-551. DOI: 10.1126/science.1220366.

Zhang X., Church J.A. (2012) Sea level trends, interannual and decadal variability in the Pacific Ocean. Geophysical Research Letters 39: n/a-n/a. DOI: 10.1029/2012gl053240.

Zhang, X., J. Church, S. Platten, and D. Monselesan (2014) Projection of subtropical gyre circulation and associated sea level changes in the Pacific based on CMIP3 climate models, Climate Dynamics, 43(1-2), 131-144.

Appendix: Sea Level Projections and Allowances at the Coastal Council Scale

The sea level and allowance data provided to Tasmanian Department of Premier and Cabinet are based on the Climate Change in Australia data sets described in McInnes et al. (2015) and references therein. These data have been interpolated to approximately the locations of the coastal councils around Tasmania corresponding with coastal council boundaries and relevant islands. Spatial information on the extent of council boundaries was sourced from the https://data.gov.au website in the form of shape polygons.

For the calculation of allowances, a list of scale parameters (λ), with corresponding latitudes and longitudes were sourced from the hydrodynamic modelling study of Haigh et al. (2014). These scale parameters were available at approximately every 8 km along the coast. Scale parameters were also sourced for the set of tide gauge locations as discussed in Hunter et al., (2013). For each point of a coastal council boundary polygon, the location of the closest scale parameter was identified. For all scale parameters identified within 5.5 km of the coastal boundary points, the minimum, maximum and median scale parameters and their associated locations were identified. When no scale parameters resided within 0.05° of the council's coastal points, the search area was extended to 1° (~111 km). Examples included King and Flinders islands in Bass Strait.

Sea level data were sourced from the gridded historical regional sea level dataset of Church and White (2011) and gridded regional projections of Church et al. (2013). Both of these data sets were on a 1° by 1° grid. The sea level data were extracted from the nearest grid point in these data sets to the coastal council boundary points. The projections are after a 21-year average has been applied to the annual values, removing much of the interannual variability.

CONTACT US

t 1300 363 400
+61 3 9545 2176
e enquiries@csiro.au
w www.csiro.au

AT CSIRO WE SHAPE THE FUTURE

We do this by using science to solve real issues. Our research makes a difference to industry, people and the planet.

As Australia s national science agency we ve been pushing the edge of what s possible for over 85 years. Today we have more than 5,000 talented people working out of 50 plus centres in Australia and internationally. Our people work closely with industry and communities to leave a lasting legacy. Collectively, our innovation and excellence places us in the top ten applied research agencies in the world.

WE ASK, WE SEEK AND WE SOLVE

FOR FURTHER INFORMATION

Oceans and Atmosphere
Kathleen McInnes
t +61 03 9239 4569
e Kathleen.McInnes@csiro.au
w http://www.cmar.csiro.au/sealevel/